



ELSEVIER

Journal of Crystal Growth 231 (2001) 8–16

JOURNAL OF  
**CRYSTAL  
GROWTH**

www.elsevier.com/locate/jcrysgro

# A comparative study of surface reconstruction of wurtzite GaN on (0001) sapphire by RF plasma-assisted molecular beam epitaxy

Kyeong K. Lee<sup>a,\*</sup>, William A. Doolittle<sup>a</sup>, Tong-Ho Kim<sup>a</sup>, April S. Brown<sup>a</sup>, Gary S. May<sup>a</sup>, Stuart R. Stock<sup>b</sup>, Zu Rong Dai<sup>b</sup>, Zhong L. Wang<sup>b</sup>

<sup>a</sup>*School of Electrical and Computer Engineering, Georgia Institute of Technology, Atlanta, GA 30332-0250, USA*

<sup>b</sup>*School of Material Science and Engineering, Georgia Institute of Technology, Atlanta, GA 30332-0250, USA*

Received 27 November 2000; accepted 7 March 2001

Communicated by T.F. Keuch

## Abstract

We present a comprehensive study of the electrical, optical, and structural properties of wurtzite GaN films grown under various initial growth conditions. The GaN films were grown directly on sapphire substrates using GaN nucleation layers by a Riber 3200 system with a radio-frequency plasma source. In situ reflection high-energy electron diffraction (RHEED) reveals a strong correlation between nucleation conditions, including the nitridation step, and the final surface reconstruction of the GaN thin film. Well-defined reconstruction patterns, primarily  $(2 \times 2)$  and  $(4 \times 4)$ , are observed for some of the nucleation conditions. Hall mobility, photoluminescence (PL), X-ray rocking curve data, and transmission electron microscopy (TEM) measurements are used to interpret the observed relationship. The results show that for the conditions investigated, an unreconstructed  $(1 \times 1)$  surface after growth correlates with improved electrical, optical, and structural properties. The surface reconstructed thin film exhibits a strong columnar growth with inversion domains (IDs). We attribute the degraded characteristics to the presence of a mixture of both polarities in the films with reconstruction. © 2001 Published by Elsevier Science B.V.

*PACS:* 81.05.Ea; 81.15.Hi; 61.14.Hg; 61.72.Ef

*Keywords:* A1. Surface structure; A3. Molecular beam epitaxy; B1. Gallium compounds; B1. Sapphire

## 1. Introduction

Reconstruction patterns obtained using reflection high-energy electron diffraction (RHEED) are often used to establish proper growth conditions

for various compound semiconductors during molecular beam epitaxy (MBE), especially the well-established GaAs- and InP-based materials. However, the understanding of GaN reconstruction patterns in relation to material characteristics is still developing.

Several surface reconstructions have been observed for wurtzite GaN, and specific

\*Corresponding author.

*E-mail address:* kl45@prism.gatech.edu (K.K. Lee).

reconstructions are thought to be correlated with improved growth conditions for obtaining high quality epitaxial GaN layers [1–9]. Iwata et al. reported that improved photoluminescence and X-ray diffraction characteristics of GaN on sapphire correlate with a  $(2 \times 2)$  reconstruction [4]. A report by Hacke et al. [5] for GaN epitaxial layers grown on metal organic chemical-vapor deposition (MOCVD)-grown GaN template layers indicates that stronger  $(2 \times 2)$  reconstructions—far from the transition regime from unreconstructed  $(1 \times 1)$  toward reconstructed  $(2 \times 2)$ —leads to inferior electrical properties. Structural and optical properties were not discussed.

Most of these studies were performed by growing GaN films on MOCVD-grown GaN templates [1,2,5,7,8]. Generally, limited sample quantities were used to extract the correlations. A series of work by Smith et al. [7] has related families of reconstructions to the polarity of the GaN. The  $(1 \times 1)$  unreconstructed surface is observed on N-face GaN, while the  $(2 \times 2)$  is observed on Ga-face GaN.

In this paper, we report observed correlations between the initial growth stage (or buffer layer) conditions and surface reconstructions observed after epitaxial growth. A comparison of wurtzite GaN films grown directly on sapphire substrates, with and without surface reconstruction, is presented based on Hall effect, photoluminescence (PL), and X-ray rocking curve measurements, as well as transmission electron microscopy (TEM).

## 2. Experimental details

Growth experiments were performed in a Riber 3200 MBE system using a Oxford CARS radio frequency plasma source to supply the active nitrogen flux. For the present study, six factors for the initial stage of GaN growth were examined: time and temperature for nitridation, buffer growth temperature, Ga cell temperature, growth time, and nitrogen plasma power during buffer growth. For the nitrogen source during these steps, the flow rate was fixed at 1.63 sccm, resulting in beam equivalent pressure (BEP) of  $3.2 \times 10^{-5}$  Torr.

The traditional approach to determining relationships between growth conditions and material properties has rested on the standard experimental technique of varying one factor at a time while holding the others constant. This simple approach is effective in deriving information when the coupling of the various growth parameters is small. However, this approach does not effectively allow the observation of important interactions, which is very common in MBE growth [12,13]. In this study, we employed a computer-generated statistical experimental design technique called D-optimal design [19]. While a full-factorial design would require  $3^6$  (216) experiments to examine 3 levels for each factor, the D-optimal technique enables us to use only 30 experiments, including two center points. The detailed experimental conditions are shown in Table 1.

To separate the influence of the epitaxial layer growth conditions on the final characteristics from those of the initial growth factors, we fixed the epitaxial layer growth conditions. These conditions were a substrate temperature of 770°C, a Ga BEP of  $4.4 \times 10^{-7}$  Torr, a nitrogen flow rate of 1.63 sccm (corresponding BEP of  $3.2 \times 10^{-5}$  Torr), and a nitrogen power of 450 W. To exclude the possibility of impurity-induced reconstructions such as hydrogen, an elemental nitrogen source was used. We have no discernible source of hydrogen, excluding the possibility of hydrogen-related surface reconstructions [10,11,15]. Furthermore, the order in which experiments were performed has been randomized so as to statistically average out the effects of extraneous factors which may be present, but not considered in this study. It is known that the randomization of the experimental order helps to distinguish the change due to primary controlled operating conditions from a systematic change in machine operating conditions [14].

The temperature of the tantalum-backed sapphire substrates was measured with a pyrometer. Deposition rates were typically 0.34  $\mu\text{m}/\text{h}$ . Total film thickness, as measured using a stylus microprofilometer, ranged from 0.65  $\mu\text{m}$  to 0.75  $\mu\text{m}$ , depending on the buffer thickness. Although all six factors may affect a change in electrical, structural and optical properties, our statistical analysis

Table 1  
Experimental initial growth conditions for wurtzite GaN growth on (0001) sapphire

Run ID no.	Nitridation time (min)	Nitridation temp. (°C)	Buffer temp. (°C)	Ga flux ( $10^{-7}$ Torr)	Nitrogen Pow. (W)	Buffer time (min)
N200	1	600	400	2.1	500	3
N201 <sup>a</sup>	1	800	600	1.1	500	3
N202 <sup>a</sup>	1	600	400	1.1	350	3
N203	30	600	600	1.1	350	3
N204 <sup>a</sup>	30	800	600	1.1	500	15
N205	15.5	800	600	1.6	425	9
N206 <sup>a</sup>	1	800	400	2.1	350	3
N207 <sup>a</sup>	1	700	600	1.1	350	9
N208	30	600	600	2.1	350	15
N209	30	600	400	2.1	350	3
N210	15.5	700	500	1.6	500	3
N211 <sup>b</sup>	30	800	400	2.1	350	15
N212	1	700	600	1.6	425	15
N213 <sup>a</sup>	1	800	400	1.1	500	15
N214 <sup>a</sup>	1	800	500	1.1	350	15
N215 <sup>a</sup>	30	800	400	1.1	350	3
N216	30	600	600	2.1	500	3
N217 <sup>c</sup>	30	600	400	2.1	500	15
N218 <sup>a</sup>	15.5	600	600	1.1	500	15
N219 <sup>b</sup>	1	600	600	2.1	350	3
N220	30	800	600	2.1	350	3
N221 <sup>b</sup>	30	800	400	2.1	500	3
N222 <sup>d</sup>	1	600	500	1.6	500	9
N223 <sup>e</sup>	30	600	400	1.1	500	3
N224 <sup>c</sup>	30	600	400	1.1	350	15
N238	1	600	400	2.1	350	15
N242	30	700	500	2.1	425	9
N243 <sup>b</sup>	1	800	600	2.1	500	15
N244	15.5	700	500	1.6	425	9
N246 <sup>a</sup>	15.5	700	500	1.6	425	9

<sup>a</sup>(2 × 2) just after growth termination.

<sup>b</sup>Weak (2 × 2) observed at substrate temperature ~350°C.

<sup>c</sup>Weak (4 × 4) observed at substrate temperature ~350°C.

<sup>d</sup>(4 × 4) just after growth termination.

<sup>e</sup>(2 × 2) during growth.

revealed that nitridation time, nitridation temperature, and gallium flux (or growth rate/thickness) during low-temperature buffer growth were responsible for the majority of the variations. Dispersion of the measurements under the same conditions came from the less significant three growth conditions, which are not discussed here to avoid the complex issues associated with the simultaneous change in those six initial conditions, and so as to clarify the crucial role of the first three factors.

Note that we grew these films under nitrogen-rich (N-rich) conditions to minimize the variations of epitaxial layer quality due to the high sensitivity of morphology and related characteristics that may result from small changes in Ga flux and substrate temperature for Ga-rich growth. In addition, a limited Ga migration length ensures that the final surface morphology reflects the morphology of the buffer. We note that the assignment of the N-rich growth regime is based on our growth calibration runs. At this elevated

temperature of 770°C with the same nitrogen flow conditions, we have not observed the characteristic gallium droplets up to two-fold increase in Ga flux, indicating N-rich regime.

In situ RHEED measurements were performed using a 9 keV electron gun. Electrical characteristics of the films were measured by the van der Pauw method. Indium contacts were utilized as the ohmic contacts to GaN films. For optical characterization, PL measurements were performed using SPEX 1404 0.85 m double spectrometer with a 325 nm He–Cd laser as an excitation source. The structural properties of the films were also compared using X-ray rocking curves recorded with a Bede QC2—a double axis diffractometer equipped with a Cu tube. The detailed structural properties are examined by the cross-sectional TEM images using a JEOL 4000EX electron microscope.

### 3. Results and discussion

We observed a range of strong surface reconstructions during and just after the completion of growth, and weak reconstruction at low temperature following cooling. A few reconstructions—including  $(2 \times 2)$ ,  $(2 \times 4)$ , and  $(4 \times 4)$  reconstructions after growth, and  $(1 \times 3)$  reconstruction during nitridation—were observed in the present experiments, in addition to  $(1 \times 1)$  unreconstructed surfaces. A few samples also showed surface reconstruction 20–30 min after cooling down to a substrate temperature of about 200–300°C.

Typical RHEED patterns for unreconstructed and reconstructed wurtzite GaN are shown in Fig. 1. Fig. 1(a) and (b) show the typical  $(2 \times 2)$  reconstructed pattern along the  $[2\bar{1}\bar{1}0]$  and  $[\bar{1}\bar{1}00]$  azimuth, respectively. Although we have mostly observed the surface reconstructions after the completion of growth, these  $(2 \times 2)$  images were obtained in the midst of growth after the deposition of about 5000 Å of GaN. Fig. 1(c) and (d) also shows the  $(4 \times 4)$  reconstructed patterns obtained at  $\sim 350^\circ\text{C}$  during cooling after termination of growth. These patterns appear to be a slight variation of  $(2 \times 2)$ , since this higher-order

transition always followed the preceding  $(2 \times 2)$  lower-order reconstruction [25,26].

The  $(2 \times 2)$  reconstructions that were observed primarily after growth originated from low Ga flux during low-temperature buffer growth, together with short nitridation time and high nitridation temperature. Due to the complexity of the design of experiment method, initial growth dependencies can be best viewed in terms of the percentage of observed cases for each growth condition, as shown in Fig. 2. As can be seen in the figure, there were considerable differences in the percentage of reconstructions observed, especially for different nitridation times and Ga fluxes. As stated before, we observed the  $(2 \times 2)$  reconstruction during growth in only one case. Based on our previous growth experience both with sapphire and lithium-gallate ( $\text{LiGaO}_2$ ) substrates, however, observing  $(2 \times 2)$  surface reconstruction during growth is not rare. The GaN films grown on the cation face of  $\text{LiGaO}_2$ , which tend to grow with Ga-polarity, readily show this reconstruction during growth.

Unreconstructed  $(1 \times 1)$  surfaces were the most stable, and lasted throughout the growth period without blurring or developing spots on the diffraction lines. These stable growth fronts were obtained with high Ga flux during the buffer in conjunction with long low-temperature nitridation conditions. After a long nitridation time at low temperature, blurry but distinctive RHEED patterns corresponding to an AlN and/or AlNO layer, as evidenced by a wider rod spacing than that of the initial sapphire surface, were readily observed from the nitridated substrate. This leads us to the conclusion that a good template for the subsequent buffer layer growth was well established during this nitridation step. On the other hand, the reconstructed RHEED patterns typically came after an insufficient nitridation step as deduced by no change in rod spacing. At the onset of buffer growth, these RHEED patterns were highly unstable—the small spots gradually merge together, forming the seemingly chevroned transmission spots along the diffraction lines during the rest of the buffer growth. This suggests that under these conditions the reconstruction is related to an inferior nucleation process. Further evidence of

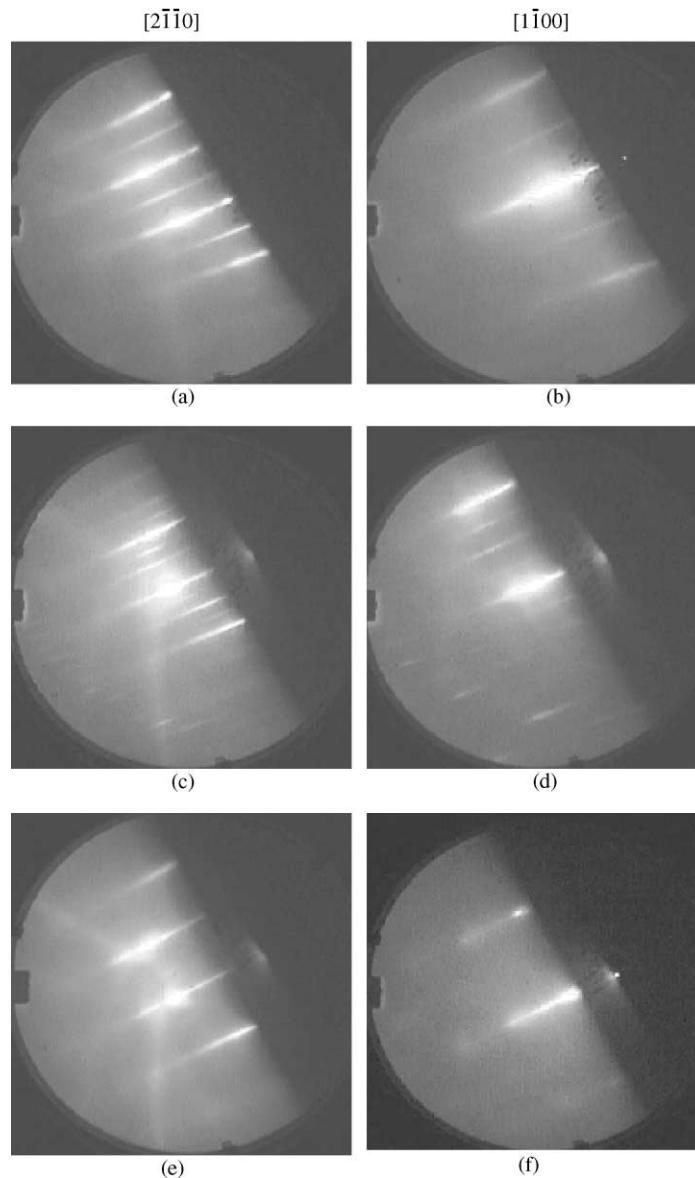


Fig. 1. Representative RHEED patterns recorded during this study. (a) and (b) for typical  $(2 \times 2)$  reconstruction, (c) and (d) for  $(4 \times 4)$  pattern, and (e) from the typical unreconstructed film.

surface roughness-related transmission features in RHEED patterns can be found in another report in which atomic force microscopy images were discussed in conjunction with nucleation conditions [20].

Hall mobility measurements were conducted at room temperature (295 K) using the van der Pauw

method. The characteristics of a total of 30 GaN samples showed Hall mobilities of 20–240  $\text{cm}^2/\text{V/s}$ , with an average n-type Si doping of  $2.1 \times 10^{18}/\text{cm}^3$ . The distribution of Hall mobility as a function of Ga flux is shown in Fig. 3. As can be clearly seen in this figure, all the films showing a unreconstructed surface following growth had

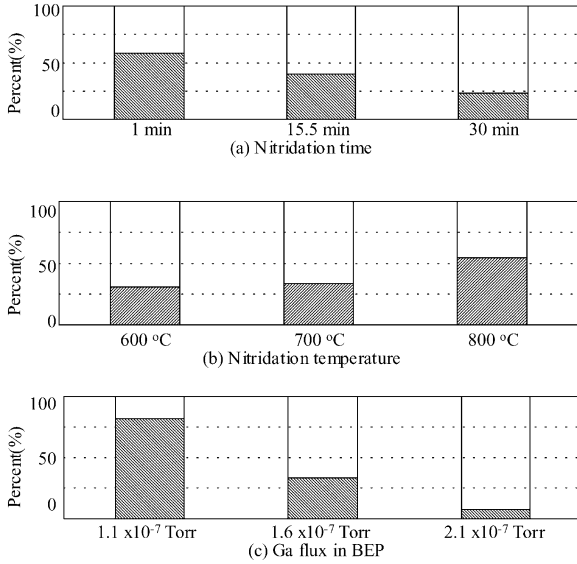


Fig. 2. Percent occurrence of reconstruction patterns including (2 × 2) and (4 × 4) at each level of the experimental conditions observed in this study as a function of (a) nitridation time, (b) nitridation temperature, and (c) Ga flux in BEP.

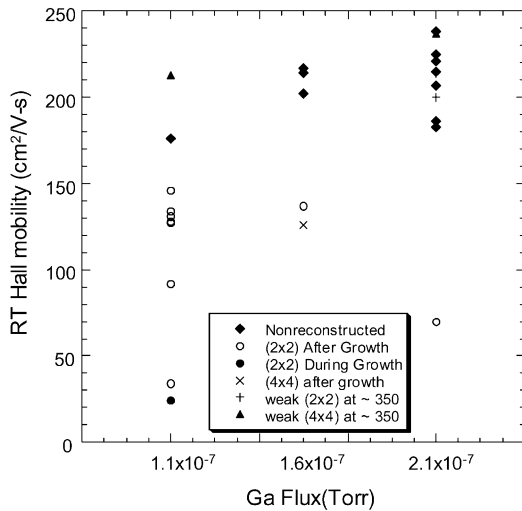


Fig. 3. Room temperature Hall mobility vs. Ga flux in BEP for surface reconstructed and unreconstructed films indicated by the open circles and closed squares, respectively.

improved mobilities. Furthermore, the transition from reconstructed to unreconstructed surfaces most likely takes place around a Ga flux of  $1.6 \times 10^{-7}$  Torr BEP (corresponding to the

growth rate of 0.2 ML/s). Moreover, as designated in the figure, the film showing a (2 × 2) reconstruction during growth had similar material properties to those (2 × 2) films observed after the termination of growth. The trend in the low-temperature reconstructed samples follows that of the unreconstructed data. Thus, we believe that the low-temperature reconstructions reflect surface population changes only. We note that, for these samples having carrier concentration  $\sim 10^{18}/\text{cm}^3$ , the electron mobility is primarily controlled both by the ionized impurity scattering mechanism and dislocation scattering [16,17]. The screening effect by excess carriers could conceal the influence of charged dislocations, leading to difficulties in explaining the correlation between the observed degradation of the material quality and the nucleation layers. However, since we manipulated only the nucleation layer growth conditions, we believe that the observed variation in carrier concentration and mobility values stems from variations in the nucleation layer, which is known to establish dislocation density and structure, as well as polarity.

Fig. 4 illustrates the characteristics of 77 K photoluminescence collected from all samples studied in this work. Donor-bound excitonic transition peaks at  $3.47 \pm 0.001$  eV were obtained

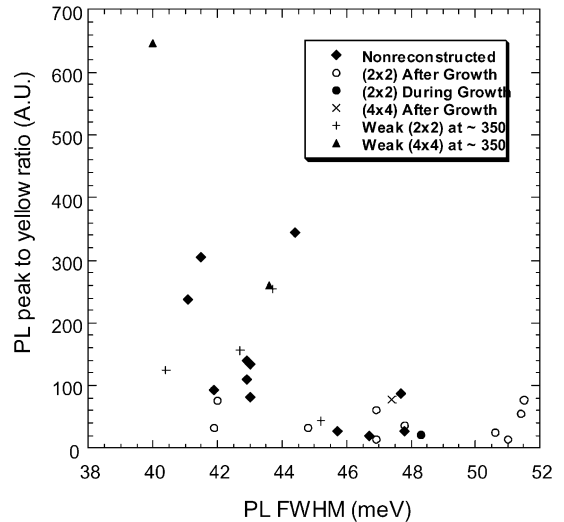


Fig. 4. 77 K photoluminescence characteristics for films with and without surface reconstruction.

from these films using a 325 nm He–Cd laser as an excitation source. Broad PL line widths observed are an evidence of poor quality material, again suggesting the inferior quality of the films with reconstruction. Those films showing surface reconstructions, grown under Ga-poor, low-temperature buffers with short nitridation times, had relatively high yellow luminescence peaks as compared to most of the unreconstructed films that were grown under Ga-rich, high-temperature buffers with long nitridation times. In this investigation, the analysis based on the relative intensity ratio between band edge and yellow luminescence was not as distinctive as the results of the electron Hall mobility data or structural characteristics as determined by X-ray diffraction.

However, we observed unique features that appeared to be correlated with the material quality. From the observed PL spectra, a point worth mentioning is that the samples having strong  $(2 \times 2)$  reconstructions typically showed two prominent peaks just below the band edge emission region at around 379 (3.271 eV) and 390 nm (3.189 eV) at 77 K measurement (not shown here). There have been a few interpretations, including that of a donor–acceptor pair (D–A), possibly due to the incorporation of undesirable impurities, or a donor bound exciton transition related to cubic inclusions in the predominantly wurtzite film [18,19]. Although we have no reliable interpretation for these transitions, we believe these are closely related to the nucleation conditions.

The structural properties of the films were also compared using X-ray diffraction recorded with a Bede QC2—a double axis diffractometer equipped with a Cu tube. Fig. 5 shows the full-width at half-maximum (FWHM) of the  $(10.5)$  vs.  $(00.4)$  reflections after correction for  $K_{\alpha 1}$  and  $K_{\alpha 2}$  dispersion. Similar to the Hall and photoluminescence observations, the FWHM was largest for samples with reconstructed surfaces, also indicating an inferior crystalline structure.

Cross-sectional TEM observations show a dramatic difference in the microstructure between a reconstructed GaN film and an unreconstructed one, as shown in Fig. 6(a) and (b). For TEM investigation, two representative samples are

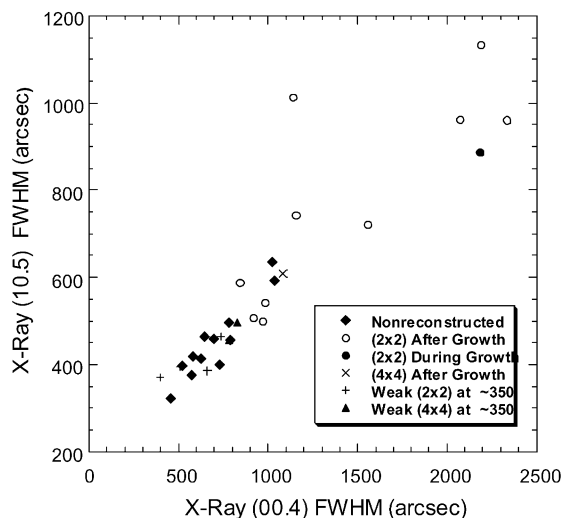


Fig. 5. A comparison of X-ray FWHM of  $(10.5)$  and  $(00.4)$  reflections showing the relatively inferior quality of reconstructed films.

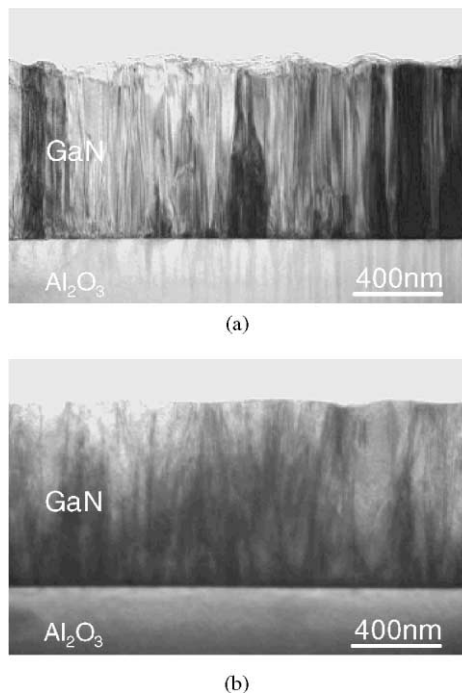


Fig. 6. Cross-sectional TEM image of the reconstructed film after growth (a) and the unreconstructed film (b). For the case of the reconstructed film, the TEM image shows a pronounced column structure having a large number of IDs. Also, the surface for the reconstructed film (a) shows many hillocks.

selected from Table 1. GaN films showing the  $(2 \times 2)$  reconstruction possess a high density of columnar structures terminating as hillocks on the surface. The high degree of defects can be seen near the interface region of the  $(2 \times 2)$  reconstructed sample. The dominant defects in this region include stacking faults, cubic inclusions, dislocations as well as inversion domains. Those columns originating from the GaN-sapphire interface extend up to the surface. Thus, the major defects of the subsequent GaN epitaxial layer are due to boundaries of inversion domains, shown in Fig. 6(a). Also, hillocks close to the top surface are prominent. The size of the hillocks of the  $(2 \times 2)$  reconstructed sample is estimated to be about  $0.2 \mu\text{m} - 0.5 \mu\text{m}$  based on AFM measurement over  $5 \mu\text{m} \times 5 \mu\text{m}$  area [20]. In general, it is known that the GaN growth rate on the Ga-polar domain is higher than that on the N-polar domains due to higher Ga surface diffusion length in the Ga-polar regime, thereby leading to hillock formation [22–24].

In contrast to the  $(2 \times 2)$  reconstructed films, the TEM image of unreconstructed  $(1 \times 1)$  films show a different microstructure in which the primary defects are dislocations, as shown in Fig. 6(b). These dislocations seem to form to relieve strain for compromising a large lattice mismatch between  $(0001)$  GaN and  $(0001)$  sapphire of  $\sim 13\%$ . The surface of unreconstructed films show a relatively flat morphology with a larger grain size than those of  $(2 \times 2)$  reconstructed films. Thus, these two different defect structures could explain the observed variation of material qualities from other measurements.

We note that our attempts to determine the polarity of the films showing reconstructions by etching in a 5 mole sodium hydroxide (NaOH) solution for 12 min were inconclusive. Specifically, etch rates of  $\sim 8.3 \text{ \AA}/\text{min}$  for  $(2 \times 2)$  reconstructed and  $\sim 25 \text{ \AA}/\text{min}$  for unreconstructed were similar enough for us to refrain from the assignment of polarity to each film. However, we note here that according to Hellman [15], the etch rate for Ga-polar material was  $< 10 \text{ \AA}/\text{min}$ , and  $\sim 100 \text{ \AA}/\text{min}$  for the N-polar case. Thus, we conclude that the films used in this study are a mixture of both types of polarities, as evidenced by the presence of IDs.

In conjunction with the surface reconstruction model of Smith et al., we believe that the inferior quality of the films with reconstruction resulted from a mixture of both polarities [7,11] and grain boundaries. This assignment is also in agreement with a recent publication by R. Dimitrov et al., who showed that mixed polarity films can result from thin layers of AlN used as a buffer, and the mixed polarity films have lower mobilities in 2DEG structures than only N-polarity films [21]. Thus, while predominant Ga face films are optimum and exhibit  $(2 \times 2)$  reconstruction, a mixed polarity films showing  $(2 \times 2)$  reconstructed film are inferior to  $(1 \times 1)$  predominant N-face films. Caution is necessary to use reconstruction as a sufficient condition for good quality.

#### 4. Summary

In summary, we present a comprehensive study of the electrical, optical, and structural properties of wurtzite GaN films grown under conditions that produce  $(2 \times 2)$  reconstructed and  $(1 \times 1)$  unreconstructed surfaces after growth. Based upon the above electrical, optical, and structural measurements under the broad range of conditions examined in this study, we conclude that an unreconstructed  $(1 \times 1)$  surface correlates with improved properties in comparison to mixed polarity films showing  $(2 \times 2)$  reconstructions. The observed differences between the unreconstructed GaN films and the reconstructed ones originates from the presence of the inversion domains associated with columnar structure, resulting in inferior quality GaN films.

#### Acknowledgements

This work was supported by DARPA/AFOSR under Grant F49620-95-1-0527.

#### References

- [1] M.E. Lin, S. Strite, A. Agarwal, A. Salvador, G.L. Zhou, N. Teraguchi, A. Rockett, H. Morkoc, Appl. Phys. Lett. 62 (1993) 702.

- [2] W.C. Hughes, W.H. Rowland Jr., M.A.L. Johnson, S. Fujita, J.W. Cook Jr., J.F. Schetzina, J. Ren, J.A. Edmond, *J. Vac. Sci. Technol. B* 13 (1995) 1571.
- [3] R.J. Molnar, R. Singh, T.D. Moustakas, *J. Electron. Mater.* 24 (1995) 275.
- [4] K. Iwata, H. Asahi, S.J. Yu, K. Asami, H. Fujita, M. Fushida, S. Gonda, *Jpn. J. Appl. Phys.* 35 (1996) L289.
- [5] P. Hacke, G. Feuillet, H. Okumura, S. Yoshida, *Appl. Phys. Lett.* 69 (1996) 2507.
- [6] W.S. Wong, N.Y. Li, H.K. Dong, F. Deng, S.S. Lau, C.W. Tu, J. Hays, S. Bidnyk, J.J. Song, *J. Crystal Growth* 164 (1996) 159.
- [7] A.R. Smith, R.M. Feenstra, D.W. Greve, M.S. Shin, M. Skowronski, J. Neugebauer, J.E. Northrup, *Appl. Phys. Lett.* 72 (1998) 2114.
- [8] O.H. Hughes, D. Korakakis, T.S. Cheng, A.V. Blant, N.J. Jeffs, C.T. Foxon, *J. Vac. Sci. Technol. B* 16 (1998) 2237.
- [9] E.C. Piquette, P.M. Bridger, Z.Z. Bandic, T.C. McGill, *Mat. Res. Soc. Symp. Proc.* 512 (1998) 387.
- [10] W.E. Packard, J.D. Dow, K. Doverspike, R. Kaplan, R. Nicolaides, *J. Mater. Res.* 12 (3) (1997) 646.
- [11] A.R. Smith, R.M. Feenstra, D.W. Greve, M.S. Shin, M. Skowronski, J. Neugebauer, J.E. Northrup, *J. Vac. Sci. Technol. B* 16 (4) (1998) 2242.
- [12] M. Sherwin, G. Munns, M. Elta, E. Woelk, S. Crary, L. Terry, G. Haddad, *J. Crystal Growth* 111 (1991) 594.
- [13] R. Bicknell-Tassius, K. Lee, A. Brown, G. Dagnall, G. May, *Appl. Phys. Lett.* 70 (1) (1997) 52.
- [14] G.E. Box, N.R. Draper, *Empirical Model-Building and Response Surfaces*, Wiley, New York, 1987.
- [15] E. Hellman, *MRS Internet J. Nitride Semicond. Res.* 3 (1998) 11.
- [16] N.G. Weimann, L.F. Eastman, D. Doppalapudi, H.M. Ng, T.D. Moustakas, *J. Appl. Phys.* 83 (7) (1998) 3656.
- [17] H.M. Ng, D. Doppalapudi, T.D. Moustakas, N.G. Weimann, L.F. Eastman, *Appl. Phys. Lett.* 73 (6) (1998) 821.
- [18] P.A. Grudowski, A.L. Holmes, C.J. Eiting, R.D. Dupis, *Appl. Phys. Lett.* 69 (24) (1996) 3626.
- [19] A.V. Andrianov, D.E. Lacklison, J.W. Orton, D.J. Dewsnip, S.E. Hooper, C.T. Foxon, *Semicond. Sci. Tech.* 11 (1996) 366.
- [20] K.K. Lee, W.A. Doolittle, A.S. Brown, G.S. May, S.R. Stock, *J. Vac. Sci. Technol. B* 18 (3) (2000) 1448.
- [21] R. Dimitrov, M. Murphy, J. Smart, W. Schaff, J.R. Shealy, L.F. Eastman, O. Ambacher, M. Stutzmann, *J. Appl. Phys.* 87 (7) (2000) 3375.
- [22] J. Rouviere, M. Arlery, R. Niebuhr, K. Bachem, O. Biot, *Mater. Sci. Eng. B* 43 (1997) 161.
- [23] L. Romano, J. Northrup, M. O'Keefe, *Appl. Phys. Lett.* 69 (16) (1996) 2394.
- [24] D. Cherns, W. Young, F. Ponce, *Mater. Sci. Eng. B* 50 (1997) 76.
- [25] W. Doolittle, T. Kropenwicki, C. Carter-Coman, S. Stock, P. Kohl, N. Jokerst, R. Metzger, S. Kang, K. Lee, G. May, A. Brown, *J. Vac. Sci. Tech. B* 16 (1998) 1300.
- [26] W. Doolittle, S. Kang, A. Brown, *Solid State Elect.* 44 (2000) 229.